Spectroscopic access to single-hole energies in InAs/GaAs quantum dots

E. Siebert, T. Warming, A. Schliwa, E. Stock, M. Winkelnkemper, S. Rodt, and D. Bimberg
Institut für Festkörperphysik, Technische Universität Berlin, Hardenbergstr. 36, 10623 Berlin, Germany
(Received 25 January 2009; revised manuscript received 20 April 2009; published 28 May 2009)

We present a purely spectroscopic way to determine single-particle energy level splittings in individual InAs/GaAs QDs. The method is based on a combination of μ-photoluminescence spectroscopy (μPL) with resonant excitation and μ-photoluminescence excitation spectroscopy (μPLE) of charged QDs. The approach allows elimination of all contributions from few-particle interactions such that true single-particle energy level distances are determined. For the present InAs/GaAs QDs, showing ground-state recombination energies between 1.23 to 1.27 eV, the splitting between the hole ground state (h_0) and first excited state (h_1) is $\Delta(h_0h_1)=(27.1\pm1.8)$ meV. The splitting between the first and second excited hole states is $\Delta(h_1h_2)=(10.8\pm0.3)$ meV. These values are in good agreement with results from eight-band $\mathbf{k}\cdot\mathbf{p}$ calculations on lens-shaped InAs/GaAs QDs. Theoretical investigations identify unambiguously the heavy-hole-light-hole coupling as the decisive parameter leading to a nonzero h_1-h_2 splitting.

DOI: 10.1103/PhysRevB.79.205321 PACS number(s): 71.70.Gm, 73.21.La, 78.67.Hc

I. INTRODUCTION

Semiconductor quantum dots (QDs) possess a discrete electronic structure[1,2] in contrast to continuous bands of energy levels in bulk semiconductors. The eigenenergies and wave functions of the three-dimensionally confined electrons and holes were calculated in the past as a function of size, shape, and chemical composition of the QDs by semiempirical pseudopotential theory[3,4] and eight-band $\mathbf{k}\cdot\mathbf{p}$ theory[5,6] including first- and second-order piezoelectric effects.

In optical experiments on ensembles of QDs the luminescence or absorption of millions of excitonic complexes is observed, leading to contourless inhomogeneously broadened lineshapes. Advanced experimental techniques such as cathodoluminescence,[7] μ-photoluminescence spectroscopy (μPL),[8,9] and μ-photoluminescence excitation spectroscopy (μPLE)[10–13] enabled spectroscopic investigations of single excitonic complexes such as excitons, biexcitons, trions, and the study of few-particle effects as a function of geometry and chemical compositions of the QDs.[14,15] In order to compare with theoretical predictions the single-particle theory had to be further extended to a theory of few particles by taking into account direct Coulomb exchange and correlation effects. Only very recently a proper treatment of exchange effects was proposed,[16] enabling a quantitative comparison with experiments. A direct test of single-particle calculations by comparison to optical experiments is desirable but still missing.

A memory concept based on hole storage in valence energy levels of a few QDs has been proposed recently.[17,18] The storage capability in such a memory structure is decisively influenced by the hole-level structure of QDs.

In this paper, we present a purely spectroscopic method to determine directly the single-particle energy level splittings in individual InAs/GaAs QDs. We will focus here on hole levels. Results of μPL with resonant excitation and μPLE experiments on the positively charged trion $X+$ ($e_0h_0h_0$) are compared to each other. In the μPLE spectra the four-level fine structure of the hot trion $X+^*$ ($e_0h_0h_1$) is visualized.[16,19,20] The relaxation to the ground state $X+$ of one of the hot trion states is blocked due to a parallel spin orientation of the hole spins and Pauli's principle. That leads to additional direct recombination processes in this relaxation-blocked state. The observation of these recombination processes enables the direct measurement of the single-particle hole-level splittings. As the initial state of the recombination processes equals the final state of the corresponding excitation process, all few-particle effects are eliminated by subtracting both energies. The single-particle hole-level energy splittings $\Delta(h_0h_1)$ and $\Delta(h_1h_2)$ are obtained with high accuracy. If μPLE investigations of the X- were performed, the same approach would hold for the measurement of excited electron levels.

II. EXPERIMENTAL

The investigated QDs were grown by molecular-beam epitaxy (MBE) on GaAs(001) substrate. For the QD layer nominally 2.5 monolayers of InAs are deposited and covered by GaAs at 485 °C. The QD density is on the order of 5×10^{10} cm^{-2} with the PL maximum at 1.12 eV [full width at half maximum (FWHM) of 75 meV]. For the single QD measurements, we choose QDs with an exciton ground-state recombination energy between 1.23 and 1.27 eV on the high energy side of this distribution. All measurements are performed at 15 K. The QD luminescence is excited by a tunable cw Ti:Sapphire laser through a gold shadow mask with 100 and 200 nm apertures on the sample surface and detected by a triple 0.5 m monochromator with a LN_2-cooled charge coupled device (CCD).

III. SINGLE LEVEL SPLITTING VIA OPTICAL SPECTROSCOPY

Systematic excitation-density and polarization-dependent μPL measurements enabled the identification of the emission lines corresponding to the ground-state recombination of the exciton ($X\rightarrow0$) and the positively charged trion ($X+\rightarrow h_0$).[15,21,22] The μPLE spectrum detected on the recombination energy of the positive trion $E_{\mathrm{det}}(X+\rightarrow h_0)$ in

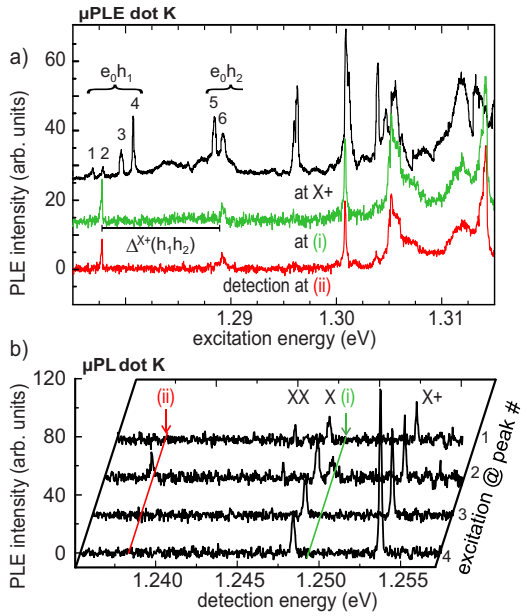

FIG. 1. (Color online) (a) μPLE spectra detected on the trion ground-state ($X+$) recombination energy and the two recombination channels, (i) and (ii), of the relaxation-blocked hot trion state. (b) μPL spectra with resonant excitation at the peak energies labeled 1–4 in (a). At resonant excitation into peak 2 additional recombination peaks emerge at detection energies of (i) and (ii). The μPL graphs are shifted vertically and horizontally for clarity.

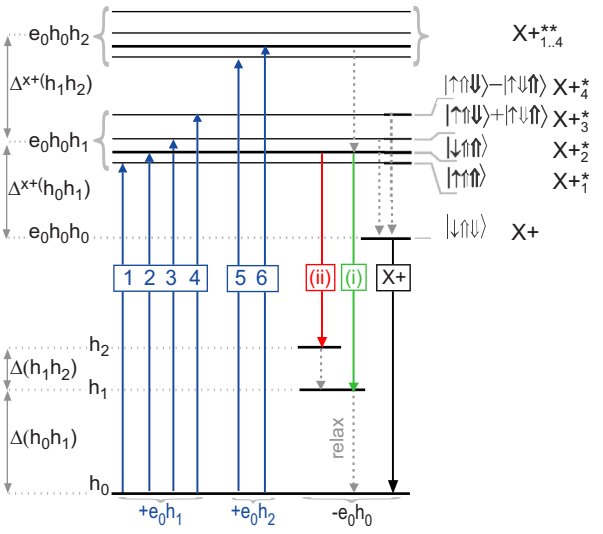

FIG. 2. (Color online) Level scheme of the $X+^{*}$ and $X+^{**}$ with the respective e_0h_1 and e_0h_2 excitations into the hot trion states $X+^{*}_{1\ldots4}$ and $X+^{**}_{1,2}$. All states of $X+^{*}$ and $X+^{**}$ are twofold degenerate. On the left-hand side the main electron-hole configuration of each excitonic complex, on the right one of the two spin configurations, is shown. Arrowheads $\uparrow$, $\Uparrow$, and $\Updownarrow$ represent the spin orientation of electrons, holes, and excited holes. Excited state relaxation pathways, according to spin-selection rules, are marked by dotted gray arrows. The three utilized recombination pathways are illustrated. Rightmost the decay of the ground-state trion $X+$. Beside the decay of the relaxation-blocked $X+^{*}_{2}$ with remaining h_1 and h_2, respectively. Excitation transitions 2 and 6 to the relaxation-blocked excited trion states are highlighted.

Fig. 1(a) reveals resonant e_0h_1 and e_0h_2 absorption lines of a QD charged with a hole in the ground state h_0. The peak intensities reflect the transition probability of these absorption processes, the relaxation into the ground state $X+$, and its subsequent recombination. The unambiguous identification of the resonances labeled 1–4 to $h_0 \rightarrow X+^{*}_{1\ldots4}$ excitations into the four states of the hot trion $X+^{*}$ in the configuration $e_0h_0h_1$ was enabled by a comparison to the fine-structure splitting of the $X+^{*}$ revealed by the decay of the positively charged biexciton in μPL.[16] A deviation from QD structures with mathematically exact symmetry is indicated by the observation of e_0h_1 transitions. As all three particles of the $X+^{*}$ occupy different orbitals, the exchange interaction between them leads to a fine-structure splitting of the energy levels resulting in four twofold degenerate sublevels, denoted as $X+^{*}_{1\ldots4}$ (see Fig. 2).[19,20,23–25] The $X+^{*}_{1}$, $X+^{*}_{2}$, and $X+^{*}_{3}$ states are triplet states with the projection of total angular momentum $F_z = \pm 7/2$, $F_z = \pm 5/2$, and $F_z = \pm 1/2$, respectively. $X+^{*}_{4}$ is a singlet state with $F_z = \pm 1/2$. For each state one of the two possible spin configurations is shown in Fig. 2. The spin orientation of the electrons (heavy holes) is denoted with $\uparrow\downarrow \pm 1/2$ ($\Downarrow\Uparrow \pm 3/2$), whereby bold arrowheads ($\Downarrow\Uparrow$) mark the spin orientation of holes in the excited state. For simplicity only the isotropic contributions of the exchange interaction and heavy-hole states are considered.

Resonances 5 and 6 in Fig. 1(a) correspond to $h_0 \rightarrow X+^{**}_{1,2}$ excitations into the first two states of the excited trion $X+^{**}$ ($e_0h_0h_2$), as will be shown later in this work. The $X+^{**}$ is expected to exhibit a fundamentally similar fine structure to $X+^{*}$ of four twofold degenerate states, as shown in Fig. 2. The absolute magnitude of the $X+^{**}$ fine-structure splitting deviates from that of the $X+^{*}$ since it is determined by the spatial extent of the three wave functions.

In order to interpret the relative intensities of peaks 1–4, spin-selection rules for an e_0h_1 absorption are considered. Thus, an estimate for the probability of excitations $h_0 \rightarrow X+^{*}_{1\ldots4}$ into each of the four $X+^{*}_{1\ldots4}$ states and their relaxation probability into the $X+$ ground state can be given. Conservation of total angular momentum $\Delta F_z = \pm 1$ demands that the absorbed electron and hole must have opposite spins, e.g., $|\uparrow\Downarrow\rangle$. Then, the e_0h_1 absorptions to the $X+^{*}_{2}$ and to the $|\uparrow\Uparrow\Downarrow\rangle$ part of the $X+^{*}_{3}$ and $X+^{*}_{4}$ are optically allowed. Absorption to the $|\uparrow\Downarrow\Uparrow\rangle$ part of the $X+^{*}_{3}$ and $X+^{*}_{4}$ states, as well as to the $X+^{*}_{1}$ state is forbidden. Consequently the spin-dependent e_0h_1-absorption probability is one for $X+^{*}_{2}$, one half for $X+^{*}_{3}$ and $X+^{*}_{4}$, and zero for $X+^{*}_{1}$. Experimentally absorption resonances 1–4 exhibit an intensity ratio of $I(1):I(2):I(3):I(4) = 0.18:0.17:0.50:0.64$ (mean values for six dots). The theoretical estimate of the absorption probability approximately agrees for intensities $I(1)$, $I(3)$, and $I(4)$ even though heavy-hole-light-hole mixing and the anisotropic part of the exchange interaction soften the derived optical selection rules.[16] However, *the deviation of* $I(2)$ from its theoretical value is striking. This peak intensity does not only reflect the absorption but also the relaxation efficiency from $X+^{*}_{2}$ to the $X+$ level, (cf. Fig. 2). As the holes in the ground and first excited states have parallel spins in $X+^{*}_{2}$, the relaxation of the excited hole is blocked. Long-time constants for hole spin flips in InAs/GaAs QDs[26,27] lead to the reduced intensity of

$I(2)$ and an increased probability for an e_0h_0 recombination in the relaxation-blocked state $X+_2^*$.

Two recombination channels of the relaxation-blocked state $X+_2^*$, dubbed as (i) and (ii) throughout this work, were observed. They are disclosed by two additional peaks being present in the μPL spectrum [Fig. 1(b)] upon resonant excitation at the energy corresponding to the transition $h_0 \rightarrow X+_2^*$ (peak 2). These emission lines are not visible at excitation energies in resonance to the other three transitions $h_0 \rightarrow X+_{1,3,4}^*$.

In order to identify these two recombination channels, the μPLE spectra detected at the recombination energy of both channels will be analyzed now. In addition, this analysis will enable an estimate of the hole p-state splitting.

The excitation spectra detected on the emission line of recombination channels (i) and (ii) are displayed in Fig. 1(a). Their correspondence with several resonances in the excitation spectrum detected on the trion ground state $X+$, which is observed for all investigated QDs, shows that identical excited states from the same QD are probed here. Moreover, the excitation spectra detected at (i) and (ii) share exactly the same signature, proving that a radiative recombination from the same state of the QD is probed. However, the detection energies have a separation of 11.0 meV pointing to different final states for the two recombination processes. As expected from the μPL graphs, both excitation spectra have a common resonance at the energy of the peak labeled 2 in the excitation spectrum detected on the ground-state recombination energy of $X+$. Thus, the $h_0 \rightarrow X+_2^*$ excitation results in three different emission lines. One corresponds to the radiative e_0h_0 recombination in $X+$ after relaxation. Two emission lines are related to the direct e_0h_0 recombination in the relaxation-blocked state $X+_2^*$. The same three emission lines are observed for excitation in resonance with peak 6 in Fig. 1(a). This resonance belongs to an excitation to the next optically active excited trion level, which might be formed either by a $e_1h_0h_0$ or a $e_0h_0h_2$ configuration. Higher indexed configurations are unlikely due to the small energy difference of 11.4 meV between peaks 2 and 6. Only the e_0h_2 excitation generates an excited trion with a fine structure and a relaxation-blocked state. Therefore, resonance 6 is assigned to the transition $h_0 \rightarrow X+_2^{**}$. Here, $X+_2^{**}$ corresponds to an excited trion state in the configuration $e_0h_0h_2$ having a total angular momentum $F_z = \pm 5/2$. On that basis peak 5 can be interpreted as an $h_0 \rightarrow X+_1^{**}$ excitation to the state with total angular momentum $F_z = \pm 7/2$. These transitions are illustrated in Fig. 2 by arrows numbered 5 and 6. A correct assignment of any two peaks in the excitation spectrum to transitions into the excited trion states $X+_3^{**}$ and $X+_4^{**}$ is not feasible at this point.

Still, the μPLE results reflect the energy level splitting between the excited trions $X+^*$ and $X+^{**}$ in the configurations $e_0h_0h_1$ and $e_0h_0h_2$. That splitting deviates from the single-particle energy level splitting of the excited hole states h_1 and h_2 due to few-particle effects, such as direct Coulomb and exchange interactions. The contribution of the Coulomb interaction to both binding energies is similar as the wave functions of the excited holes h_1 and h_2 of $X+^*$ and $X+^{**}$ both have a leading p-orbital character.[4,28,29] Furthermore, the influence of exchange effects is minimized for the observed energy difference of 11.4 meV between peaks 2 and 6 since excited trion states with the same main total angular momentum $\pm 5/2$ are considered. Overall, the energy separation $\Delta^{x+}(h_1h_2) := E_{\mathrm{exc}}(h_0 \rightarrow X+_2^{**}) - E_{\mathrm{exc}}(h_0 \rightarrow X+_2^*)$ between resonances 2 and 6 should deviate only little from the true p-state splitting $\Delta(h_1h_2)$ between the single-particle hole states h_1 and h_2. See also notes in Refs. 30 and 31.

Knowing now the approximate hole p-state splitting $\Delta^{x+}(h_1h_2)$ enables the identification of the two direct recombination processes, (i) and (ii). As the initial state for both recombination processes is identical, the difference of their detection energies yields the energy level splitting between the final states, without the influence of any additional few-particle effects (cf. Fig. 2 and note in Ref. 30). Indeed, the μPL spectrum displayed in Fig. 1(b) shows that recombination channel (ii) of the relaxation-blocked state $X+_2^*$ is redshifted by 11.0 meV with respect to channel (i). That corresponds well to the $\Delta^{x+}(h_1h_2) = 11.4$ meV splitting. The small deviation reflects the differences of the Coulomb interactions between $X+^*$ and $X+^{**}$, which is included in $\Delta^{x+}(h_1h_2)$ but not in the single-particle level splitting $\Delta(h_1h_2)$. Thus, recombination channel (i) corresponds to the $X+_2^* \rightarrow h_1$ and (ii) to the $X+_2^* \rightarrow h_2$ recombination. The latter process involves an energy transfer promoting the spectator hole from the first excited hole state h_1 to the second one h_2.

For the QD, whose spectra are displayed in Fig. 1, the hole p-state splitting $\Delta(h_1h_2)$ is 11.0 meV. The single-particle level splitting $\Delta(h_0h_1)$ can now be determined based on the identification of recombination channel (i) with the transition $X+_2^* \rightarrow h_1$. The difference between the energy $E_{\mathrm{det}}(X+_2^* \rightarrow h_1)$ of the direct e_0h_0 recombination in $X+_2^*$ and the energy $E_{\mathrm{exc}}(h_0 \rightarrow X+_2^*)$ for resonantly exciting the $X+_2^*$ yields the single-particle level splitting $\Delta(h_0h_1) = E_{\mathrm{exc}}(h_0 \rightarrow X+_2^*) - E_{\mathrm{det}}(X+_2^* \rightarrow h_1)$ between the first two hole levels h_0 and h_1 of the QD (cf. Fig. 2). For the QD shown in Fig. 1 a value of $\Delta(h_0h_1) = 28.4$ meV is determined. In Table I the hole-level splittings of four additional QDs are listed, resulting in average values of $\Delta(h_0h_1) = (27.1 \pm 1.8)$ meV and $\Delta(h_1h_2) = (10.8 \pm 0.3)$ meV. The exciton ground-state transition energy for these dots differs by up to 37 meV. Such weak dependence of the hole energy levels from the ground-state energy of the QDs is expected theoretically.[5,29]

IV. THEORY

In order to support the above conclusions and to understand the origin of the observed hole-level splitting, realistic modeling based on a three-dimensional (3D) implementation of the eight-band $\mathbf{k} \cdot \mathbf{p}$ model for the single-particle states and the configuration interaction method for the exciton energies is used. The inhomogeneous strain as well as first- and second-order piezoelectric effects are accounted for. A detailed description of the entire method can be found in Refs. 5 and 6.

As model structures lens-shaped InAs/GaAs QDs, with a trumpetlike InAs composition profile as, e.g., observed in Refs. 32–34 are used. Diameters and heights range from 40–19 and 3.6–9.5 nm, respectively, whereby the total amount of InAs is kept constant. The experimentally ob-

TABLE I. Single-particle hole-level splittings compared to the energy separation $\Delta^x(h_0h_1)$, $\Delta^x(h_1h_2)$ among X, X^*, and X^{**}. The energetic difference $\Delta^{x+}(h_0h_1)$, $\Delta^{x+}(h_1h_2)$ among $X+$, $X+^*$, and $X+^{**}$ is listed as well. All energies are in meV.

	One particle		Two particles		Three particles	
$E(X)$	$\Delta(h_0h_1)$	$\Delta(h_1h_2)$	$\Delta^x(h_0h_1)$	$\Delta^x(h_1h_2)$	$\Delta^{x+}(h_0h_1)$	$\Delta^{x+}(h_1h_2)$
1228.6	28.4	10.5	28.9	10.3	25.6	11.7
1245.1	28.3	10.8	30.2	8.1	24.2	7.8
1247.4	25.6		26.9	10.2	20.9	9.9
1248.4	28.4	11.0	29.5	9.0	24.9	11.4
1265.7	24.8		27.5	7.7	20.9	9.9

served large oscillator strength for the e_0h_1 absorption processes suggests a deviation from QD structures with mathematically exact symmetry. This is taken into account by a granulated alloy of the QDs, which has been shown to give reasonable explanation for lifting of the optical selection rules in MBE grown In(Ga)As/GaAs QDs.[16] The color scheme of the upper QD in Fig. 3 presents the continuous virtual crystal approximation (VCA) of the In distribution leading to strict selection rules and thus prohibiting e_0h_1 transitions. Starting from this InAs composition a granulated alloy is derived, as shown for the lower dot in Fig. 3. For a given fraction $(x, 1-x)$ of $In_xGa_{1-x}As$ at a given grid point InAs is chosen with probability x and GaAs with $1-x$. Since the choice is not unique we applied this procedure several times for each QD. Due to the resulting granular In distribution any symmetry of the system is lifted. Consequently, the strict selection rules are lifted and the e_0h_1 transitions into the excited trion states couple to the light field, in accordance to the experimental observations.

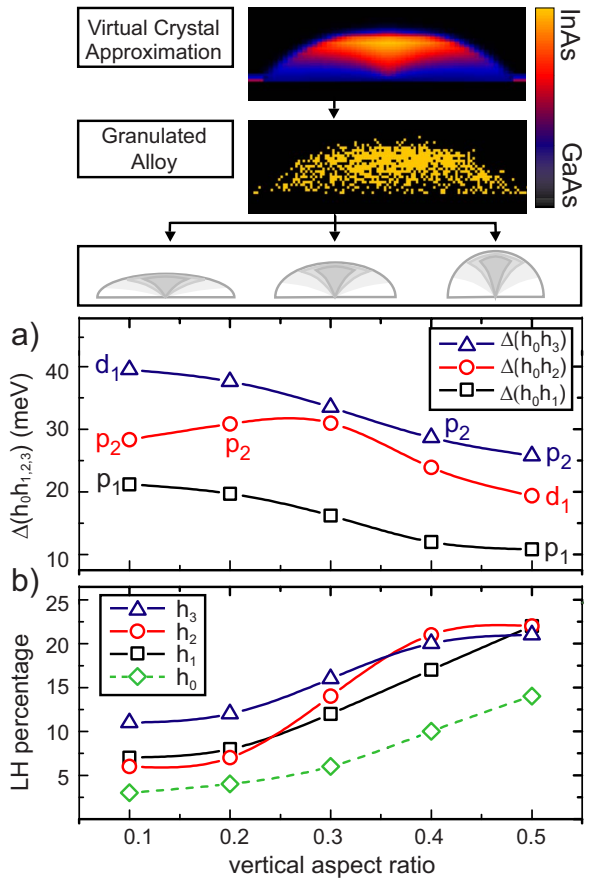

FIG. 3. (Color online) Our model QD in the VCA on the top and with a granular In distribution (non-VCA). (a) Single-particle hole-level splitting $\Delta(h_0h_1)$ and $\Delta(h_0h_2)$ for lens-shaped QDs, with diameters and heights ranging from 40–19 and 3.6–9.5 nm, respectively. The In distribution is handled in the non-VCA mode. (b) Light-hole contribution to the first four hole states h_0, h_1, h_2, and h_3.

The single-particle energy differences $\Delta(h_0h_1)$ and $\Delta(h_0h_2)$ for these structures are shown in Fig. 3(a). Values between 21.8 and 6.5 meV are observed for $\Delta(h_0h_1)$ and between 6.5 and 14.0 meV for $\Delta(h_1h_2)$. Up to an aspect ratio of 0.3 the splittings are in good agreement with the experimental values. In addition, the calculated exciton ground-state transition energies match the experimental range. For aspect ratios larger than 0.2 the second p state crosses the first d state; hence, $\Delta(h_1h_2)$ refers to a splitting between the first p state and the first d state.

The central issue is the origin of the large splitting between the first and second excited hole states, sometimes termed hole p-state splitting (although it can be a p-d splitting). In a single-band effective mass model for hole states, taking only the heavy-hole parts into account, a $C_{\infty v}$ or C_{4v} confinement symmetry results in a p-state splitting $\Delta(h_1h_2)=0$. A nonzero p-state splitting in turn can only be explained by a lowering of the confinement symmetry to at most C_{2v}. The origin of such lowering can be a piezoelectric field[5] or a QD elongation.[6]

To test whether such a conclusion holds also for an eight-band $\mathbf{k}\cdot\mathbf{p}$ approach, which *includes* heavy-hole light-hole coupling, we calculate the hole p-state splitting for lens-shaped QDs as function of the *lateral* aspect ratio, including and excluding the piezoelectric field. Hence, we separately analyze the two potential sources of lateral anisotropy separately. The volume of the QDs, with a vertical aspect ratio of 0.2 and a trumpetlike InAs composition profile, is kept constant for the calculations. We use the VCA description; therewith a circular base of the QDs leads to a C_{2v} symmetry if piezoelectricity is considered, and a $C_{\infty v}$ symmetry without piezoelectricity, as the lattice structure is not included in the eight-band $\mathbf{k}\cdot\mathbf{p}$ model. The results are shown in Fig. 4: a large p-state splitting $\Delta h_1h_2 > 7.2$ meV remains even in the case of a circular-based QD, having a $C_{\infty v}$-confinement sym-

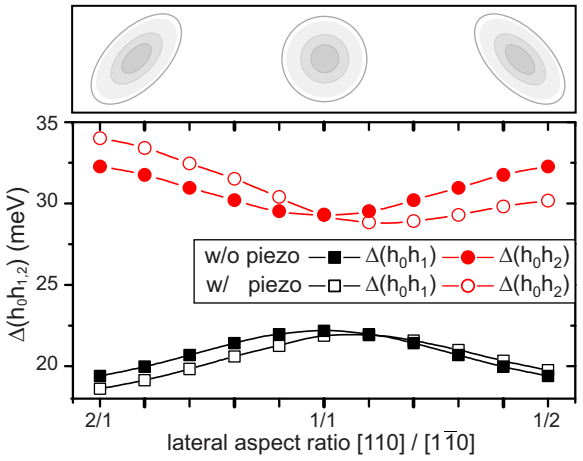

FIG. 4. (Color online) Hole-level splittings in the absence and presence of piezoelectric fields for lens-shaped QDs of varying lateral aspect ratio. The vertical aspect ratio of the QD is 0.2.

metry, in *absence* of piezoelectricity. The splitting is weakly affected by the QD elongation. Thus, the origin of the splitting is the heavy-hole-light-hole coupling in such QDs. It depends on their size and their vertical aspect ratio. The coupling is smaller in flat QDs, resulting in a smaller p-state splitting.[35] For large very flat QDs the coupling disappears, leading to a degeneracy of h_1 and h_2 (see Fig. 16 in Ref. 6).

For the nonelongated lens-shaped QDs the light-hole contribution to the hole wave functions h_i is displayed in Fig. 3(b) as a function of the vertical aspect ratio. Its percentage increases for all hole states upon larger vertical aspect ratios and is accompanied by an increase in the p-state splitting. Thus, the heavy-hole-light-hole coupling seems to rule the experimentally observed nonzero hole p-state splitting. In contrast the piezoelectric field is too small in these QDs to impose such a large hole p splitting.

V. FEW-PARTICLE EFFECTS

The exciton binding energy is experimentally not accessible. Knowing the single-particle level splittings among h_0, h_1, and h_2, the difference between the binding energies of a ground-state exciton (trion) and the exciton (trion) with one hole in the excited state can be quantitatively analyzed. Therewith, the spatial overlap of the electron (e_0) and hole (h_0,h_1,h_2) wave functions in ground and excited complexes is characterized.

The energy separation $\Delta^{x+}(h_0h_1)$ between $X+^*$ ($e_0h_0h_1$) and the ground state $X+$ ($e_0h_0h_0$) is accessible by μPLE detected on $E_{\mathrm{det}}(X+\rightarrow h_0)$. To account for the exchange interaction in $X+^*$, the mean value over all four excitation energies $E_{\mathrm{exc}}(h_0\rightarrow X+^*_{1\ldots4})$ has been taken to obtain the values of $\Delta^{x+}(h_0h_1)$ shown in Table I. Compared to $\Delta(h_0h_1)$, $\Delta^{x+}(h_0h_1)$ is shifted to lower energies. The deviation $\Delta^{x+}(h_0h_1)-\Delta(h_0h_1)$ itself is related to the variation in the Coulomb interaction (binding energy) between $X+$ and $X+^*$. Values between −2.8 and −4.7 meV demonstrate a stronger binding of the single particles in the $X+^*$ complex. The reduced attractive (repulsive) Coulomb interaction between the h_1 and

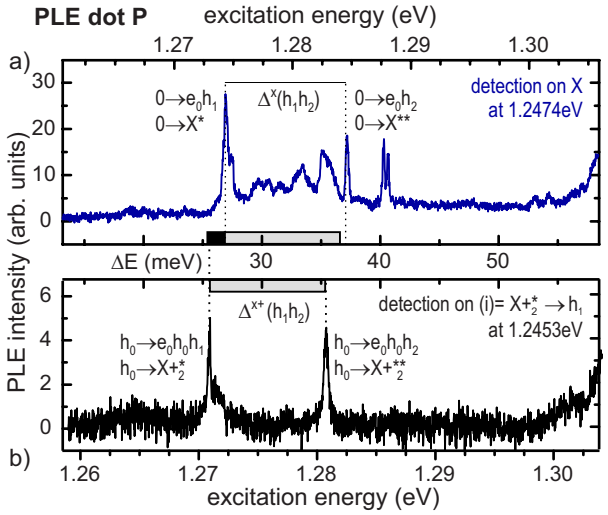

FIG. 5. (Color online) (a) μPLE spectrum detected on $E_{\mathrm{det}}(X\rightarrow0)$, showing the e_0h_1 and e_0h_2 absorptions. Labels next to the peaks indicate the corresponding transitions. (b) μPLE spectrum detected on $E_{\mathrm{det}}(X+^*_2\rightarrow h_1)$. The $\Delta^{x+}(h_1h_2)$ is in good agreement with $\Delta^{x}(h_1h_2)$ in the exciton excitation spectrum. The shared ΔE axis defines the difference between excitation and detection energy in the corresponding μPLE spectrum.

e_0 (h_0) in the $X+^*$ is a result of the leading p-orbital character of h_1.

The spatial extent of the h_1 wave function in comparison to the h_2 and h_0 wave function is accessed by an analysis of few-particle effects in the ground X (e_0h_0) and excited state excitons X^* (e_0h_1) and X^{**} (e_0h_2). Knowing the single-particle hole-level splittings, transitions into excited exciton states X^* and X^{**} can be identified in the μPLE detected on the exciton ground-state emission line $E_{\mathrm{det}}(X\rightarrow0)$. This spectrum [Fig. 5(a)] shows two resonances at the energies ΔE=26.9 and 37.3 meV above $E_{\mathrm{det}}(X\rightarrow0)$. From the excitation spectrum detected on the relaxation-blocked hot trion [Fig. 5(b)] the hole-level splittings $\Delta(h_0h_1)$=25.6 meV and $\Delta^{x+}(h_1h_2)$=9.9 meV can be determined directly. The gray bars in the upper and lower panels of the figure mark the energy $\Delta^{x+}(h_1h_2)$. This splitting is almost identical to the energy difference of 10.2 meV between the two peaks in the exciton excitation spectrum. The peaks in the exciton excitation spectrum are therefore identified as a generation of a X^* (e_0h_1) and X^{**} (e_0h_2) into an empty QD. Thus, $\Delta^{x}(h_0h_1)$ and $\Delta^{x}(h_1h_2)$ are determined to be 26.9 and 10.2 meV from Fig. 5(a).

The difference of the exciton binding energy between X and X^* of $\Delta^{x}(h_0h_1)-\Delta(h_0h_1)$=1.3 meV is marked in Fig. 5 by the black bar. The positive value points to a weaker binding of X^* compared to X. That matches theoretical results,[3–6] where h_1 has a smaller overlap with e_0 than h_0 leading to a reduction in the attractive Coulomb interaction by 1.3 meV in the e_0h_1 complex. Values between 0.5 and 2.7 meV for different QD underline this finding. For three QDs the difference $\Delta^{x}(h_0h_2)-\Delta(h_0h_2)$ of the exciton binding energy between X^{**} and X has been measured. The binding energy of X^{**} is always larger than that of X^* and for two dots even larger than that of X, as values of $\Delta^{x}(h_0h_2)-\Delta(h_0h_2)$ between

0.3 and −0.9 meV demonstrate. Thus, the spatial overlap of h_2 with e_0 is larger than the one with h_1, and for negative values of $\Delta^x(h_0h_2)-\Delta(h_0h_2)$ even larger than the one with h_0.

VI. CONCLUSION

Using a combination of μPLE and resonant μPL we have directly determined the splitting between the first three single-particle hole levels in individual QDs, eliminating all few-particle effects. For the present InAs/GaAs QDs the energy level splitting between the hole in the ground state (h_0) and the first excited state (h_1) is $\Delta(h_0h_1)=(27.1\pm1.8)$ meV. The splitting between the excited hole states is determined to $\Delta(h_1h_2)=(10.8\pm0.3)$ meV.

Resonant excitation of a relaxation-blocked hot trion state enabled the observation of two different recombination channels. The first one leaves a single hole in the first excited state of the QD after the recombination process $X+_2^*\rightarrow h_1$. The second recombination channel $X+_2^*\rightarrow h_2$ is characterized by an energy transfer to the hole in the first excited state, promoting it to the second excited state. As the relaxation is blocked for both recombination processes, the difference between the excitation energy $E_{\mathrm{exc}}(h_0\rightarrow X+_2^*)$ and the detection energy $E_{\mathrm{det}}(X+_2^*\rightarrow h_1)$ or $E_{\mathrm{det}}(X+_2^*\rightarrow h_2)$ yields $\Delta(h_0h_1)$ or $\Delta(h_0h_2)$, in accordance to the note in Ref. 30. Thus, the influence of any additional few-particle effects is eliminated.

Knowing the single-particle level splittings the variation in the binding energy within an exciton or positive trion after the transfer from the ground to an excited state is quantitatively analyzed. The binding energy of $X+^*$ is 2.8 to 4.7 meV larger than that of $X+$. For the excited excitons, X^* and X^{**}, we determine a 0.5–2.7 and 0.3–(−0.9) meV smaller binding energy compared to the ground state X. These results agree with theoretically predicted larger wave-function overlap of the e_0 with the h_2 as compared to h_1.

Calculations in the framework of the eight-band $\mathbf{k}\cdot\mathbf{p}$ model on flat lens-shaped QDs reproduced the experimentally found hole-level splittings well. The heavy-hole-light-hole coupling is unambiguously identified as the parameter causing the experimentally observed nonzero hole p-state splitting.

ACKNOWLEDGMENTS

We are indebted to A. E. Zhukov, G. E. Cirlin, and V. M. Ustinov for providing the samples. This work was partly funded by the SfB 787 of the DFG. The calculations were performed on an IBM p690 supercomputer at the HLRN Berlin/Hannover.

[1] D. Bimberg, M. Grundmann, and N. N. Ledentsov, *Quantum Dot Heterostructures* (John Wiley & Sons, Chichester, 1998).
[2] M. Grundmann, O. Stier, and D. Bimberg, Phys. Rev. B **52**, 11969 (1995).
[3] A. J. Williamson, L. W. Wang, and A. Zunger, Phys. Rev. B **62**, 12963 (2000).
[4] G. Bester and A. Zunger, Phys. Rev. B **71**, 045318 (2005).
[5] O. Stier, M. Grundmann, and D. Bimberg, Phys. Rev. B **59**, 5688 (1999).
[6] A. Schliwa, M. Winkelnkemper, and D. Bimberg, Phys. Rev. B **76**, 205324 (2007).
[7] M. Grundmann *et al.*, Phys. Rev. Lett. **74**, 4043 (1995).
[8] K. Brunner, U. Bockelmann, G. Abstreiter, M. Walther, G. Böhm, G. Tränkle, and G. Weimann, Phys. Rev. Lett. **69**, 3216 (1992).
[9] J.-Y. Marzin, J.-M. Gerard, A. Izrael, D. Barrier, and G. Bastard, Phys. Rev. Lett. **73**, 716 (1994).
[10] A. Zrenner, M. Markmann, A. Paassen, A. Efros, M. Bichler, W. Wegscheider, G. Böhm, and G. Abstreiter, Physica B **256-258**, 300 (1998).
[11] D. Gammon, E. S. Snow, and D. S. Katzer, Appl. Phys. Lett. **67**, 2391 (1995).
[12] D. Gammon, E. S. Snow, B. V. Shanabrook, D. S. Katzer, and D. Park, Phys. Rev. Lett. **76**, 3005 (1996).
[13] R. Oulton, J. J. Finley, A. I. Tartakovskii, D. J. Mowbray, M. S. Skolnick, M. Hopkinson, A. Vasanelli, R. Ferreira, and G. Bastard, Phys. Rev. B **68**, 235301 (2003).
[14] R. Seguin, A. Schliwa, S. Rodt, K. Pötschke, U. W. Pohl, and D. Bimberg, Phys. Rev. Lett. **95**, 257402 (2005).
[15] S. Rodt, A. Schliwa, K. Potschke, F. Guffarth, and D. Bimberg, Phys. Rev. B **71**, 155325 (2005).
[16] T. Warming, E. Siebert, A. Schliwa, E. Stock, R. Zimmermann, and D. Bimberg, Phys. Rev. B **79**, 125316 (2009).
[17] A. Marent, M. Geller, A. Schliwa, D. Feise, K. Pötschke, D. Bimberg, N. Akçay, and N. Öncan, Appl. Phys. Lett. **91**, 242109 (2007).
[18] M. Geller, A. Marent, T. Nowozin, D. Bimberg, N. Akçay, and N. Öncan, Appl. Phys. Lett. **92**, 092108 (2008).
[19] K. V. Kavokin, Phys. Status Solidi A **195**, 592 (2003).
[20] M. E. Ware, E. A. Stinaff, D. Gammon, M. F. Doty, A. S. Bracker, D. Gershoni, V. L. Korenev, S. C. Badescu, Y. Lyanda-Geller, and T. L. Reinecke, Phys. Rev. Lett. **95**, 177403 (2005).
[21] M. Bayer *et al.*, Phys. Rev. B **65**, 195315 (2002).
[22] J. J. Finley, D. J. Mowbray, M. S. Skolnick, A. D. Ashmore, C. Baker, A. F. G. Monte, and M. Hopkinson, Phys. Rev. B **66**, 153316 (2002).
[23] I. A. Akimov, K. V. Kavokin, A. Hundt, and F. Henneberger, Phys. Rev. B **71**, 075326 (2005).
[24] B. Urbaszek, R. J. Warburton, K. Karrai, B. D. Gerardot, P. M. Petroff, and J. M. Garcia, Phys. Rev. Lett. **90**, 247403 (2003).
[25] R. Seguin, S. Rodt, A. Schliwa, K. Pötschke, U. W. Pohl, and D. Bimberg, Phys. Status Solidi B **243**, 3937 (2006).
[26] R. Hanson, L. P. Kouwenhoven, J. R. Petta, S. Tarucha, and L. M. K. Vandersypen, Rev. Mod. Phys. **79**, 1217 (2007).
[27] D. Heiss, S. Schaeck, H. Huebl, M. Bichler, G. Abstreiter, J. J. Finley, D. V. Bulaev, and D. Loss, Phys. Rev. B **76**, 241306(R) (2007).
[28] T. Maltezopoulos, A. Bolz, C. Meyer, C. Heyn, W. Hansen, M. Morgenstern, and R. Wiesendanger, Phys. Rev. Lett. **91**, 196804 (2003).

[29] G. A. Narvaez, G. Bester, and A. Zunger, J. Appl. Phys. **98**, 043708 (2005).

[30] Few-particle energies $e(\cdot)$ can be expressed as a sum over the single-particle energies of electrons $e(e_m)$ and holes $e(h_n)$, attractive $C_{e_m h_n}$ and repulsive $C_{h_m h_n}$ Coulomb interaction and exchange and correlation energies $K(\cdot)$. For $X+^*$ that yields: $e(X+^*)=e(e_0)+e(h_0)+e(h_1)+C_{e_0 h_0}+C_{e_0 h_1}+C_{h_0 h_1}+K(X+^*)$. The transition energies E_{det} and E_{exc} for the recombination $X+^* \rightarrow h_j$ and excitation process $h_0 \rightarrow X+^*$ are defined as the difference between $e(X+^*)$ and the energy of the final $e(h_j)$ and initial $e(h_0)$ states. By subtracting both energies, $\Delta h_0 h_j := e(h_j)-e(h_0) = E_{\mathrm{exc}}(h_0 \rightarrow X+^*)-E_{\mathrm{det}}(X+^* \rightarrow h_j)$, all contributions from few-particle effects are eliminated.

[31] $E_{\mathrm{exc}}(h_0 \rightarrow X+_2^{**})-E_{\mathrm{exc}}(h_0 \rightarrow X+_2^{*})=e(h_2)-e(h_1)+(C_{e_0 h_2}-C_{e_0 h_1})+(C_{h_0 h_2}-C_{h_0 h_1})+[K(X+_2^{**})-K(X+_2^{*})]$

[32] N. Liu, J. Tersoff, O. Baklenov, A. L. Holmes, and C. K. Shih, Phys. Rev. Lett. **84**, 334 (2000).

[33] T. Walther, A. G. Cullis, D. J. Norris, and M. Hopkinson, Phys. Rev. Lett. **86**, 2381 (2001).

[34] A. Lenz, R. Timm, H. Eisele, Ch. Hennig, S. K. Becker, R. L. Sellin, U. W. Pohl, D. Bimberg, and M. Dähne, Appl. Phys. Lett. **81**, 5150 (2002).

[35] M. Scheibner, M. Yakes, A. S. Bracker, I. V. Ponomarev, M. F. Doty, C. S. Hellberg, L. J. Whitman, T. L. Reinecke, and D. Gammon, Nat. Phys. **4**, 291 (2008).